

Article

Not peer-reviewed version

Functional Characterization of ShK Domain-Containing Protein in the Plant-Parasitic Nematode *Bursaphelenchus xylophilus*

Madalena Mendonça , [Claudia S. L. Vicente](#) , [Margarida Espada](#) *

Posted Date: 6 December 2023

doi: 10.20944/preprints202312.0388.v1

Keywords: molecular plant-nematode interaction; parasitism; pinewood nematode; ShK domain-containing protein; oxidative stress



Preprints.org is a free multidiscipline platform providing preprint service that is dedicated to making early versions of research outputs permanently available and citable. Preprints posted at Preprints.org appear in Web of Science, Crossref, Google Scholar, Scilit, Europe PMC.

Copyright: This is an open access article distributed under the Creative Commons Attribution License which permits unrestricted use, distribution, and reproduction in any medium, provided the original work is properly cited.

Article

Functional Characterization of ShK Domain-Containing Protein in the Plant-Parasitic Nematode *Bursaphelenchus xylophilus*

Madalena Mendonça, Cláudia S.L. Vicente and Margarida Espada *

MED—Mediterranean Institute for Agriculture, Environment and Development & CHANGE – Global Change and Sustainability Institute, Institute for Advanced Studies, and Research, Universidade de Évora, Pólo da Mitra, Ap. 94, 7006-554 Évora, Portugal;

* Correspondence: mespada@uevora.pt

Abstract: ShK domain-containing proteins are peptides found in different parasitic and venomous organisms. From a previous transcriptomic dataset from *Bursaphelenchus xylophilus*, a plant-endoparasitic nematode that infects forest tree species, we identified 96 transcripts potentially as ShK domain-containing proteins with unknown function in the nematode genome. This study aimed to characterize and explore the functional role of genes encoding ShK domain-containing proteins in *B. xylophilus* biology. We selected and functionally analyzed nine candidate genes specific from *B. xylophilus*. *In situ* hybridization revealed expression of one *B. xylophilus* ShK in the pharyngeal gland cells, suggesting their delivery into host cells. Most of the transcripts are highly expressed during infection and showed a significant upregulation in response to peroxide products compared to the nematode catalase enzymes. We reported for the first time, the potential involvement of ShK domain genes in oxidative stress, suggesting that these proteins may have an important role protecting or modulating the reactive oxygen species (ROS) activity of the host plant during parasitism.

Keywords: molecular plant-nematode interaction; parasitism; pinewood nematode; ShK domain-containing protein; oxidative stress

1. Introduction

Plant pathogens cause severe economic and ecological problems in a wide range of crops and forestry plant species in Europe [1]. The migratory plant parasitic nematode *Bursaphelenchus xylophilus* (pinewood nematode, PWN) is a European A2 quarantine organism which causes economic damage to the forestry industry [2,3]. Pine wilt disease is caused by the PWN, which is thought to have originated in North America but was introduced in the early XX century into Asian countries [4]. Since then, many native tree species, mainly from the genus *Pinus* spp. (pine trees), from both European (Portugal; Spain) [5,6] and Asian (Japan, Korea, China, Taiwan) [7] forests were considered highly susceptible to PWN.

The interaction between plant-parasitic nematodes (PPN), with their hosts are mediated by parasitism-related proteins (named *effectors*), which are secreted proteins produced by the nematode and delivered into the host that may modify it to their own benefit and also protect itself against host defenses [8]. Due to advances in genomics and transcriptomics, several proteins of the *B. xylophilus* have been identified as important during the interaction with the host, which include different cell-wall degrading proteins, detoxification and antioxidant enzymes, and other small molecules which can facilitate nematode survival inside the host tissues, such as toxin peptides, venom-like proteins and other peptides which their function is unknown [9,10].

ShK domain-containing proteins are distributed from both plant (e.g., *Arabidopsis thaliana* and *Oryza sativa*) and animal kingdoms (e.g. *Gallus gallus*, *Xenopus tropicalis*, *Cryptosporidium parvum*) [11]. The ShK domain-containing protein is characterized by a 35/37-residue peptide toxin, and it was originally found in cnidaria species, sea anemones *Stichodactyla helianthus* [12] and *Bunodosoma granulifera* [13], being described as a potassium channel (K⁺) blocker. Collectively, a large superfamily

of proteins that contain domains resembling ShK or BgK are referred as ShKT domains [11]. The structure of ShK domain-containing is defined by six cysteines and two α -helices and three disulfide bonds (Cys1-Cys6, Cys2-Cys4 and Cys3-Cys5) [14,15]. These peptide sequences can have a single or multiple ShKT domains and can be associated with other domains [16]. Depending on the structural organization of the polypeptide, this domain is mostly associated to metalloproteases, tyrosinases, prolyl-4-hydroxylases, oxydoreductases, and peroxidases, which can combine various additional domains (e.g., epidermal growth factor-like domains, trypsin-like serine protease, or thrombospondin-type repeats) [11]. A large number of multidomain proteins from both plants and animals, like polychaets [17], marine annelids [18], and sea snails [19], have the same evolutionary highly conserved protein motif defined by the typical structural fold of ShKT [11]. The ShKT-domain containing proteins on the Phylum Nematoda is present in the free living *Caenorhabditis elegans*, with ca. 66 secreted ShKT proteins containing multiple copies of the ShK toxin domain [20], in the entomopathogenic nematode *Steinernema carpocapsae* [21,22], in the plant-parasitic nematodes *Radopholus similis* [23], *Pratylenchus penetrans* [24], *Meloidogyne javanica* [25], *Heterodera schachtii* [26], and in the animal-parasitic species *Toxocara canis* [15] and *Trichostrongylus colubriformis* [27]. In parasitic and venomous species, the peptides with ShKT domain-like have been shown to function as K^+ channels blockers [15,28–30]. In the phylum Nematoda, ShK toxins present in the animal-parasitic nematodes *Ancylostoma caninum* (AcK1) and *Brugia malayi* (BmK1) are used as a selective inhibitor of K_v channels to treat autoimmune disease [30]. In the entomopathogenic nematode *S. carpocapsae*, the presence of ShK peptides has been associated with the modulation of the host immunity during infection and their potential to be an insecticidal peptide [21,22]. In the plant-parasitic nematode *M. javanica*, ShK peptides (*MjShKT*) are highly secreted into the host cells, inhibit programmed cell death, allowing the nematode to invade and reproduce inside the host tissues [25]. K^+ channels are known to be indirectly engaged in plant defense responses through the action of reactive oxygen species (ROS) (biotic and abiotic stress responses) meaning that it is possible that the ShK toxin has a similar impact on K_v channels in plants [31,32].

The ShKT domain is a broad and diverse family present in plants and animals. Among parasitic nematodes, few studies have been performed with these proteins. In PPNs, although ShK domain-containing protein is present, their function(s) still remains unclear in the biology of the nematodes. Understanding their role may increase our knowledge on how PPN are able to modulate host plants during infection. Based on previous transcriptomic data, this study aims to characterize the functional role of specific encoding genes of ShK domain-containing proteins, highly expressed during host infection from *B. xylophilus*. We report a new putative role for ShK proteins and suggest a new target gene(s) for the molecular PWN control.

2. Results

2.1. Characterization of ShK domain-containing protein from *B. xylophilus*

The analysis of both *B. xylophilus* genome and transcriptome [9,33,34] identified 96 transcripts potentially identified as ShK domain-containing proteins with unknown function. From those, 64% of the transcripts that encode for a ShK domain-containing protein (corresponding to 62 coding sequences) have a predicted signal peptide, suggesting their involvement on the secretory pathway of PWN. Similar to other organisms, the *B. xylophilus* ShK domain-containing proteins are composed of 35-37 amino acid residues and contain six conserved cysteine residues [12], characteristic of the ShKT motif. *B. xylophilus* transcripts potentially encoding the ShK domain-containing proteins are composed with one or more ShKT domains (IPR003582), while others can be combined with other domains (Figure 1A) [11]. A previous study showed that ShK domain-containing protein architecture displays several structural positions depending on whether it is a single or multiple ShKT domain, or whether it is associated with another domain [19]. From the 96 transcripts, 25 were predicted with a single ShKT domain, 37 with multi ShKT domain (between 2 and 4) and 34 transcripts were combined with other domains (Figure 1B). The presence of different domain's architecture may suggest that these range of proteins play different functions in the nematode. In this nematode,

transcripts are associated with several domains, such as metallopeptidases M12 (IPR001506) and M14 (IPR000834), haem peroxidase (IPR019791), tyrosinase copper-binding domain (IPR002227), epidermal growth factor (EGF)-like domain (IPR000742), CUB domain (IPR000859) and others.

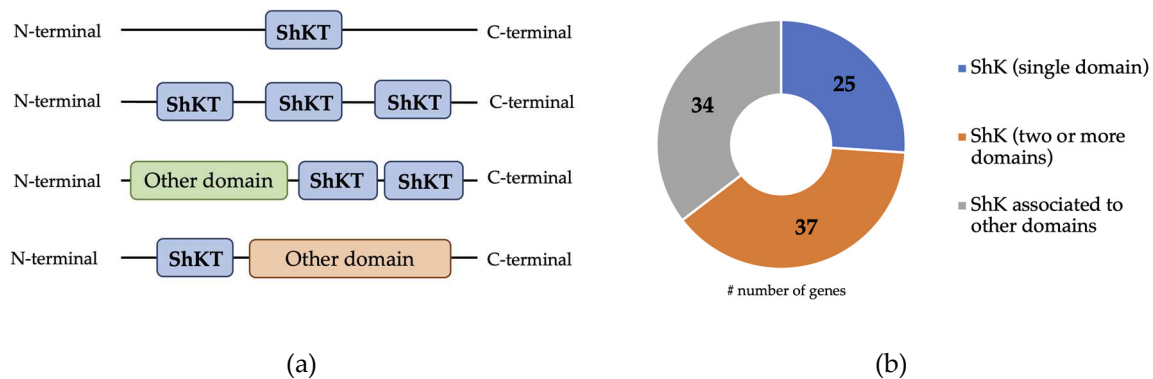


Figure 1. Representation and distribution of the main ShK domain-containing proteins predicted in *B. xylophilus*. (a) Representation of the architecture and position of the ShKT domain in ShK domain-containing proteins: one domain ShKT; multi domain ShKT and domain ShKT associated to other domain; (b) Distribution of ShK domain-containing proteins predicted in the *B. xylophilus* transcriptome.

BLASTp sequence analysis (e-value cutoff of $1e^{-5}$ and a bitscore >50) was used to identify significant matches to potential orthologs/homologs of *B. xylophilus* in Wormbase ParaSite and NCBI non-redundant databases. The results revealed that, from the total of 96 transcripts of *B. xylophilus*, 70 had a high degree of identity (50-98%) with proteins from other PPN as well as animal-parasitic and free-living nematodes, and 26 transcripts had similarity with proteins from *Bursaphelenchus spp.* Furthermore, 15 transcripts had significant sequence similarity only to *B. xylophilus* and no match to nematodes of different genera or other organisms, suggesting that these are *B. xylophilus*-specific transcripts. From these 15 ShK domain-containing proteins, 9 were selected for analysis based on the existence of a predicted signal peptide in the N-terminal and the presence of only the ShKT domain, without being associated with other domains (Figure 2A; Table 1). The sequences of the transcripts of interest in this study are BXY_0074200, BXY_0728300, BXY_1389600, BXY_0192800, BXY_0841100, BXY_1304100, BXY_1328700, BXY_1389700 and BXY_0654300. A common characteristic of these 9 transcripts is the fact that they all have two ShKT domains (D1 and D2).

2.2. *In silico* and phylogenetics analysis of the nine candidate *B. xylophilus*-specific transcripts

In silico analysis of the candidate genes revealed that the full-length DNA sequence ranged between 502 and 3250 bp, with having 1 to 4 introns, and the full length cDNA was between 423 bp and 2625 bp. The translation of the full-length cDNA revealed protein sequences between 140 to 874 amino acids (Table 1).

The expression levels of these 9 transcripts were predicted from RNA-seq data generated in a previous study [9] and the fold change for each transcript was calculated according to host infection (6 and 15 days post infection) compared with the non-parasitic stage. Most of these transcripts were highly expressed (fold change, FC >1.5) (Figure 2B), except for genes BXY_1389700 and BXY_0841100 (FC <1) that have a lower expression and BXY_1328700 that has no expression during infection. For these secreted *B. xylophilus* ShK domain-containing sequences, full length amplifications from the genomic DNA and cDNA confirmed the *in silico* prediction of the selected genes and transcripts (data not shown).

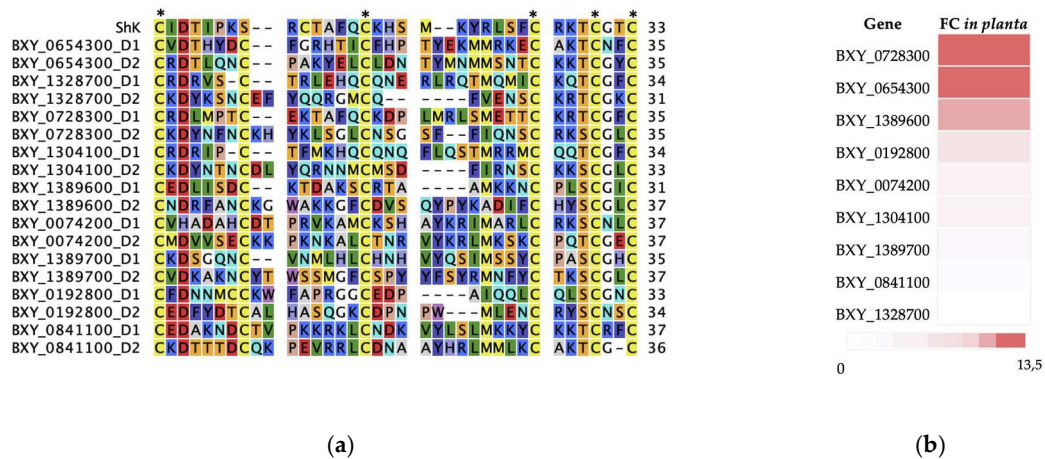


Figure 2. Characterization of the nine candidate ShK domain-containing proteins (*B. xylophilus* genes), (a) multiple sequence alignment with domain 1 (D1) and 2 (D2), and the ShKT sequence domain originally from the sea anemone *Stichodactyla helianthus*, including the six conserved cysteine residues (indicated by asterisk) which characterizes the ShKT domain; (b) representation of the ratio of the average normalized expression from the nine candidate genes, ranked by their fold change values (FC). Fold change ratio refers to the expression during infection of the host (6 and 15 days post infection) compared with a non-parasitic stage.

Table 1. Characterization of the nine candidate genes from *B. xylophilus* selected in the present study which encode ShK domain-containing proteins. All the genes have only sequence similarity to the species *B. xylophilus* and no other organisms. These genes encode for two ShK domain-containing proteins and have the presence of a signal peptide (SP). Gene (GL), number of introns (IN), transcript length (TL) and protein size (PS) were predicted for each candidate gene. Sequence similarity and percentage of homology (%) were predicted with BLASTP (closest homologue in nr database is indicated by the NCBI accession number).

Gene ID	GL*	IN	TL*	PS**	SP	Sequence similarity ID (NCBI accession number)	BLAST e-value
BXY_0192800	630	2	510	169	Yes, 1-17	[CAD5228099.1] <i>Bursaphelenchus xylophilus</i> , 100%	4e-123
BXY_0728300	502	1	429	142	Yes, 1-16	[CAD5230694.1] <i>Bursaphelenchus xylophilus</i> , 100%	6e-94
BXY_1389600	534	1	492	163	Yes, 1-21	[CAD5234029.1] <i>Bursaphelenchus xylophilus</i> , 100%	1e-111
BXY_0074200	447	0	447	148	Yes, 1-22	[CAD5228719.1] <i>Bursaphelenchus xylophilus</i> , 100%	3e-105
BXY_0841100	1170	2	669	229	Yes, 1-17	[CAD5208706.1] <i>Bursaphelenchus xylophilus</i> , 100%	8e-157
BXY_1304100	922	1	423	140	Yes, 1-16	[CAD5233070.1] <i>Bursaphelenchus xylophilus</i> , 100%	2e-98
BXY_1328700	673	1	444	147	Yes, 1-23	[CAD5233069.1] <i>Bursaphelenchus xylophilus</i> , 100%	3e-99
BXY_0654300	3250	4	1926	641	Yes, 1-20	[CAD5235767.1] <i>Bursaphelenchus xylophilus</i> , 100%	<0
BXY_1389700	3240	2	2625	874	Yes, 1-21	[CAD5234030.1] <i>Bursaphelenchus xylophilus</i> , 100%	<0

* basepairs; ** aminoacids.

To perform the phylogenetics analysis, we aligned the sequence domains of the nine candidate transcripts specific to *B. xylophilus* with sequence domains from other nematodes and plants (Supp. data Table S1). The multiple sequence alignment revealed that ShKT D1 domain sequences were more similar to each other than with ShKT D2 domain, and vice versa. Therefore, two separate Maximum likelihood (ML) phylogenetic trees were constructed (Figure 3). Both ML trees showed similar topology with: ShKT domains of plants as outgroup (*A. suecica* KAG7546197 and *Eucalyptus grandis* XP_010033232) a sub-clade formed with animal-parasitic species *B. malayi* (VIO92324) and *T. canis* (KHN87551), and free-living nematodes *B. okinawaensis* (CAD5214648) and *Diploscapter pachys* (PAV73547). In fact, the complete protein sequences of these domains shared between them other domains, such as di-copper centre-containing and tyrosinase domains with several identical sequences associated with the ShKT domain. A second sub-clade grouped the nine *B. xylophilus* domains with with *Strongyloides ratti* (CEF69303) (animal-parasitic) and *C. elegans* (CCD70350) (free-living), both with two ShKT domains (D1 and D2) the same as the candidate genes. The ShKT D1 domain-tree also showed a sub-cluster with *M. incognita* (Minc3s00855g18130) and *H. glycines* (Hetgly.G000014452) (plant-parasitic) with a significant bootstrap (higher than 90%) sharing a single ShKT domain. Some candidate genes (BXY_0192800 D1, BXY_0074200 D1, BXY_1389600 D1, BXY_1389700 D1, BXY_0654300 D1, BXY_0192800 D2, BXY_1389700 D2, BXY_1389600 D2) have a low bootstrap (< 40%), it is not possible to infer their relation in the tree. These data may suggest that these *B. xylophilus* specific genes could be obtained independently from the others, and not evolving as a result of duplication of a single ancestor.

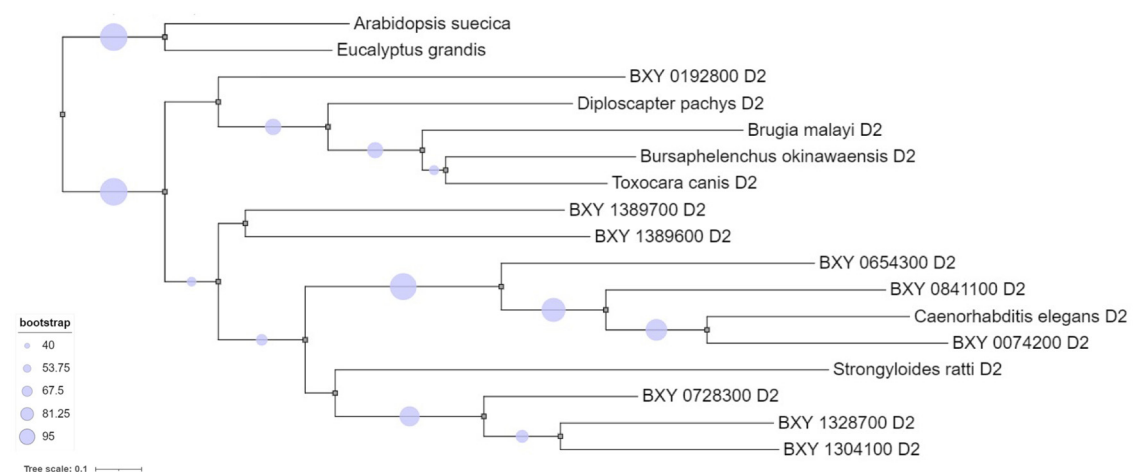
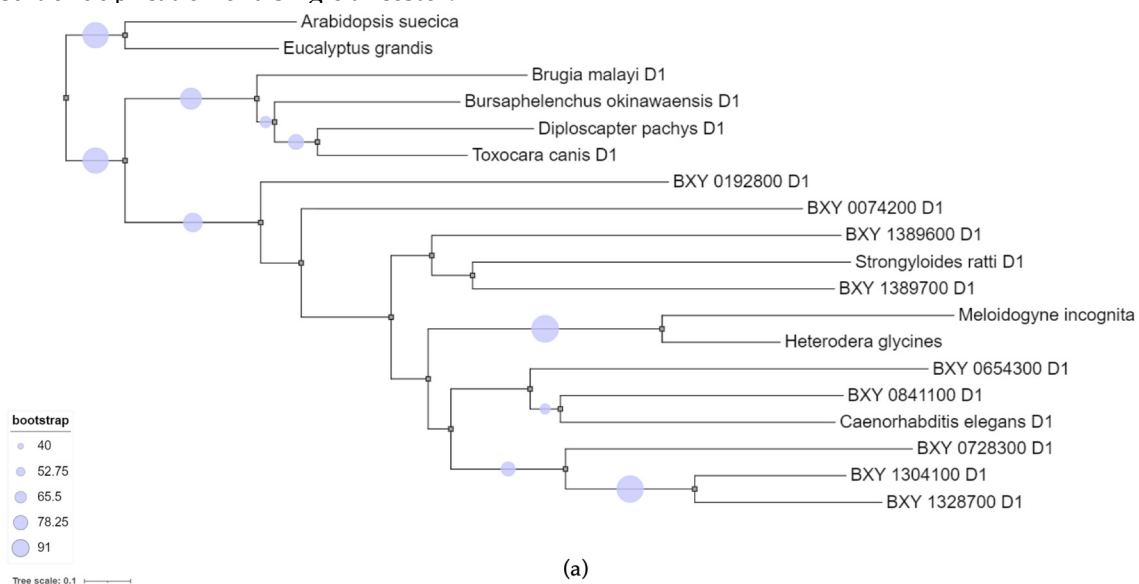


Figure 3. Maximum-likelihood (ML) phylogenetic tree that represents the protein sequence similarity between of the nine candidate genes specific *B. xylophilus* predicted ShK domain-containing proteins and other organisms, such as plant-parasitic, animal-parasitic and free-living nematodes and plants also ShK domain-containing proteins. (a) ML tree using domain 1 (D1) and ML tree using domain 2 (D2).

2.3. Spatial expression of the candidate ShK domain-containing proteins

In situ hybridization is often used to determine the spatial expression of the transcripts in the nematode tissues. We have studied the spatial expression patterns of the nine putatively ShK domain-containing proteins secreted proteins in mixed life stage nematodes. A positive labeling with the *anti-sense* probe localized one gene in the pharyngeal gland cells tissues (BXY_0728300) (Figure 4A), four genes in the intestine region (BXY_0654300, BXY_1389600, BXY_0074200, BXY_0192800) (Figure 4B,C,D,E) and two genes in the nervous system region (BXY_0841100 and BXY_1389700) (Figure 4). No signal was observed for the two remaining genes (BXY_1328700 and BXY_1304100) (figure not shown) and *in sense* probes used as control. These results suggest that the ShK domain-containing proteins are expressed in different tissues of the nematode, meaning that they may have diverse functions.

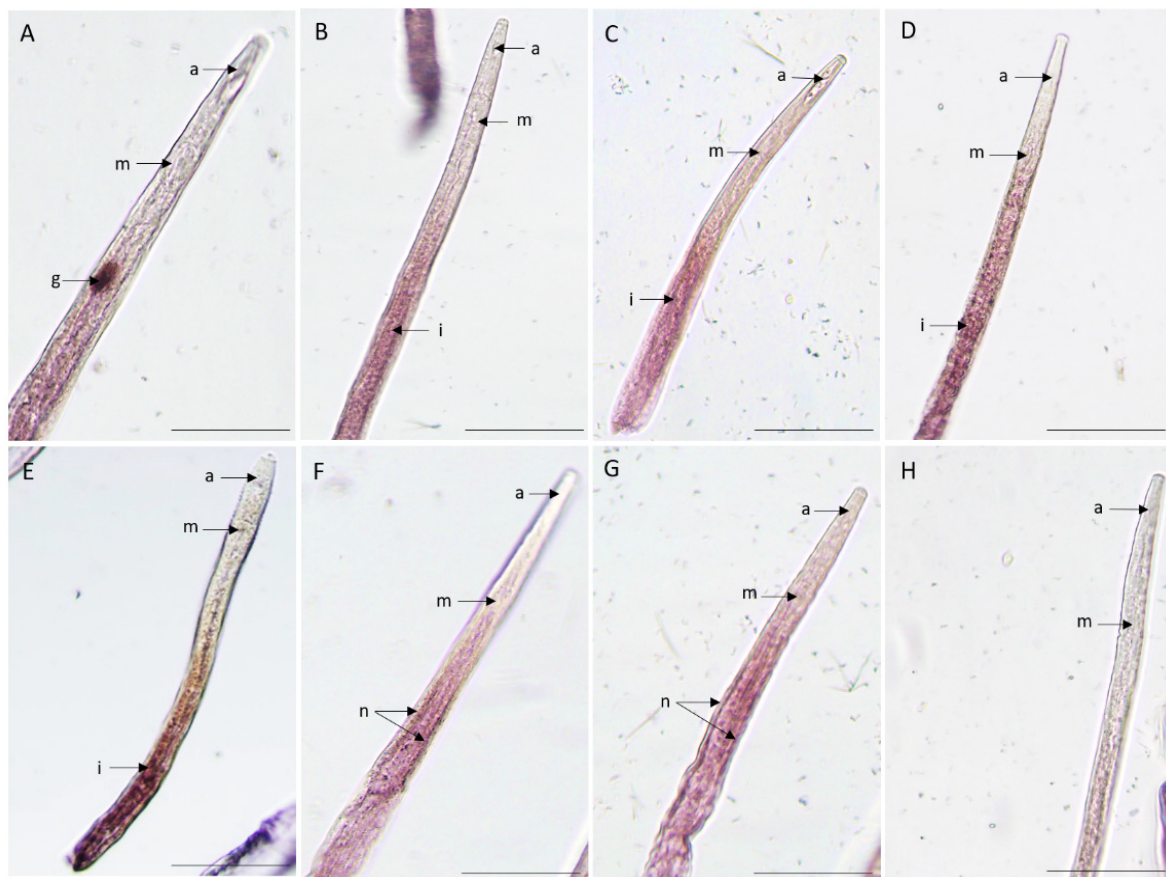


Figure 4. Detection of nine candidate genes, ShK domain-containing proteins, *B. xylophilus* transcripts by *in situ* hybridization. Transcripts were localized in different tissues of the nematode using the complementary anti-sense DIG-labeled probes. (A) BXY_0728300, (B) BXY_1389600, (C) BXY_0074200, (D) BXY_0192800, (E) BXY_0654300, (F) BXY_0654300, (G) BXY_0841100, (H) sense probe. The different nematode anterior section of the body are labeled: a: anterior region; g: pharyngeal gland cells; i: intestine region; m: median bulb; n: nervous system. Bars = 20 μ m.

2.4. High gene expression of *B. xylophilus* ShK domain-containing proteins under oxidative stress

The expression profile of the nine transcripts were validated by qRT-PCR (quantitative reverse-transcriptase PCR) under an oxidative stress test to understand their response to the presence of hydrogen peroxide (H₂O₂). The hydrogen peroxide was intended to represent the ROS products. The specificity and efficiency of all the designed primers were demonstrated in a qRT-PCR amplification, for each primer pair that had a single expected size, and the melting curves showed a single peak in the reaction. Relative expression levels for the candidate genes were compared with *B. xylophilus* catalases, *Bxy-ctl-1* (BXY_1386500) and *Bxy-ctl-2* (BXY_1745800) [35], since their biochemical function is to catalyze the reaction by which the H₂O₂ is decomposed. The results were normalized for the *B. xylophilus* reference gene, *Bx-actin*. At 15mM H₂O₂, almost all genes were significantly upregulated (ANOVA, Tukey's test; $p < 0.05$), in exception of BXY_0074200, that was downregulated, and BXY_0192800 and BXY_0841100 with no significant expression ($p > 0.05$) (Figure 5). At 30mM of H₂O₂, 11 genes showed a significant upregulation (ANOVA, Tukey's test; $p < 0.05$), except for the gene BXY_0192800 (Figure 5). Also, both *Bxy-ctl-1* (BXY_1386500) and *Bxy-ctl-2* (BXY_1745800) showed a significant expression in the two treatment conditions. These data may suggest that ShK domain-containing proteins may be participating in the response to oxidative stress and, therefore, might be important during the interaction with the host.

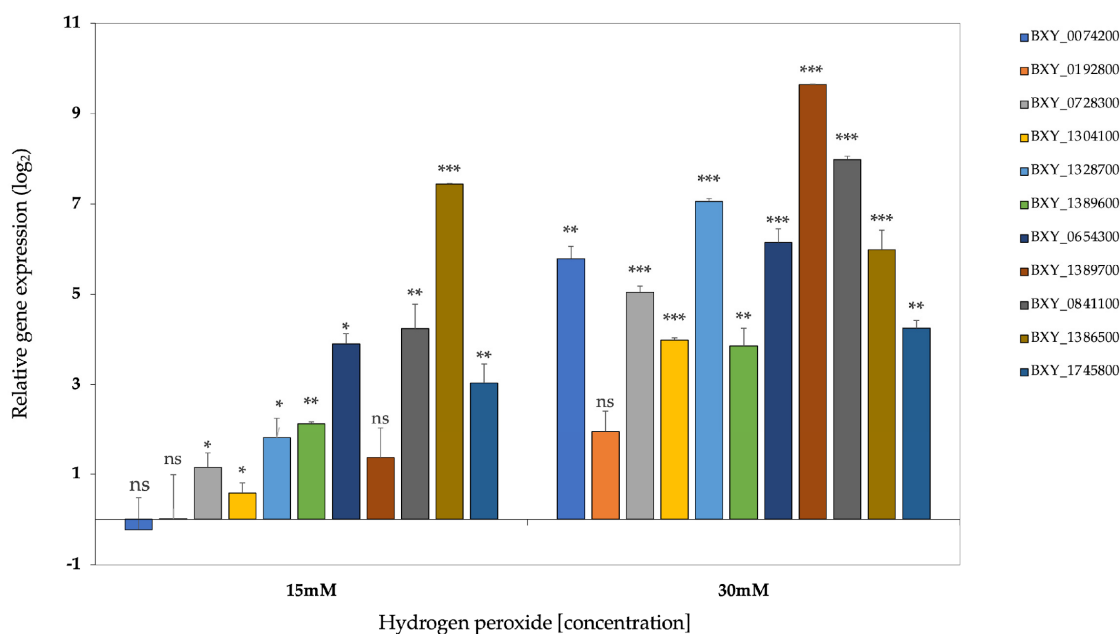


Figure 5. Normalized expression ratio (log₂) of the nine candidate genes and *Bxy-ctl-1* (BXY_1386500) and *Bxy-ctl-2* (BXY_1745800) under oxidative stress conditions (15mM and 30mM H₂O₂). Symbols on the top of the columns indicate statistical significance at (*) $p < 0.05$, (**) $p < 0.01$ and (***) $p < 0.001$ (Tukey's test) significantly different compared with the control treatment (zero). n.s. not significant.

3. Discussion

The ShK domain-containing proteins are distinguished by a conserved and small ShKT domain, distributed across animal and plant kingdoms, involving ShK toxic peptides and larger multidomain proteins with a variety of functions [11,12,19]. In this study, we have identified 96 transcripts encoding for ShK domain-containing proteins from one of the most damaging PPN, *B. xylophilus* [9,33], and showed that the putative secreted proteins were enriched in these sequences - 64% of these sequences encode a predicted signal peptide - which indicates that it might belong to secretory pathways. These proteins have been also found in the secretome of several animal parasitic nematodes (e.g. *Teladorsagia circumcincta*) [36] and other in plant parasitic nematodes, including *B. xylophilus*, *P. penetrans*, *R. similis*, *M. javanica* [23–25,37]. The number of predicted ShK sequences constitute one of the large known protein families in Nematoda (e.g., *T. circumcincta*) [16,36] which

is also observed in our data from *B. xylophilus*. Moreover, one study observed a life stage-specific regulation of the expanded gene family of ShK-domain containing proteins in the animal parasitic nematode, *T. circumcincta* [36], however for PWN this differential expression has not been observed for ShK genes [34]. All *B. xylophilus* predicted ShK domain-containing proteins sequences showed a similar structure with single or multi-domain ShKT or are associated with other protein domains as observed in other organisms (e.g., cnidaria) [38]. The number and variety of potential combinations of domains in these proteins may be an indication of the variety of functions associated.

Nine candidate species-specific genes were selected based on the presence of a predicted signal peptide and two ShKT domains (multi-domain). *In silico* analysis of these genes resulted in a lack of similarity to other sequences which indicates to be species-specific. These genes were putatively found highly expressed during infection of the host [9], suggesting that they might be involved in parasitism. Taking this information, we investigated the spatial expression profiles of these candidate transcript genes and confirmed their expression in different nematode tissues. Two gene transcripts were detected in structures of the nervous system (BXY_0841100 and BXY_1389700) and both have a lower expression during infection with the host (FC <1). The nervous system is composed of major dorsal and ventral nerves along the body of the nematode, nearly associated with the epidermis, containing cell bodies that make and receive synapses with other neurons [39]. Some parasitic related genes have been localized in nervous system tissues (e.g., *R. similis*) [23]. Curiously, a PWN catalase, which was used as a positive control for our ROS experiment, expressed in a transgenic of *C. elegans* (for *B. xylophilus* catalase, *Bxy-ctl-2*, BXY_1745800) was also localized in the nervous system [35]. Another validated gene BXY_0728300 was localized in the pharyngeal gland cells, a specialized tissue important in plant-nematode interactions. Several studies showed the relevance of pharyngeal gland cells as a producer of several proteins that are secreted and potentially related to parasitism. The ShK domain-containing proteins that has also been identified in other plant-parasitic nematodes, such as, in *P. penetrans* [24], in *R. similis* [23], *M. javanica* [25] and *H. schachtii* [26] are also expressed in the pharyngeal gland cells. *M. javanica* secreted ShK protein, *MjShKT*, is expressed in the dorsal gland cell, upregulated in parasitic stages and manipulates the plant effector-triggered immune response [25]. In addition, some genes have been expressed in other nematode tissues and still have a role in parasitism. The majority of the ShK-domain encoding genes analyzed gave a signal in the intestine (BXY_0654300, BXY_1389600, BXY_0074200, BXY_0192800), which may indicate that these genes may be involved or have a protective activity against stress-related plant molecules during migration or infection. Previous studies have shown that *B. xylophilus* has several proteins that are highly expressed during infection, and broadly expressed in the intestine, such as two catalases [35] and several detoxification enzymes (e.g., glutathione S-transferase) [40]. Therefore, this emphasizes the multilayer strategy of PWN which may have a protective role against plant defense compounds [9].

All nine ShK domain-containing protein genes showed an upregulation in the expression levels in response to the H₂O₂ at 30mM treatment, suggesting that these proteins might be responsive to H₂O₂ and indirectly involved in the ROS scavenging. We reported for the first time, the potential involvement of ShK domain genes in oxidative stress. In summary, due to its multi-domain architecture and large number, ShK domain-containing proteins may have a diversity of functions in nematodes. Previously described functions of ShK domain-containing proteins in parasitic nematodes, including those involved in immuno-modulatory action [30] or response in order to establish and maintain the feeding sites [25]. Our data suggest that the migratory endoparasitic nematode *B. xylophilus* uses highly secreted ShK domain-containing proteins to respond to ROS products, secreting into the host and at the same time in the digestive and nervous system. Understanding the role of ShK domain-containing proteins may increase our knowledge of how nematodes modulate hosts during infection and develop new target molecules for nematode control.

4. Materials and Methods

4.1. Biological material

The isolate of *B. xylophilus*, isolate HF (Herdade da Ferrara, Portugal) used in this study was cultured at NemaLab, University of Évora. The nematodes were cultured on *Botrytis cinerea* on barley seeds at 25°C [41] for approximately 10 days. Mixed life stage nematodes were harvested using the modified Baermann funnel technique [42] for 6 hours, followed by sieving (38 µm).

4.2. In silico and phylogenetics analysis of *B. xylophilus* ShK domain-containing protein sequences

A comprehensive list of 96 transcripts encoding the ShK domain-containing sequences was identified using the previous *B. xylophilus* genomic [33] and transcriptomic data [9]. Protein sequence similarity analysis was performed by BLASTp [43,44] to analyze the similarity to other amino acid sequences against NCBI NR (non-redundant) database (<https://www.ncbi.nlm.nih.gov/>). The homology of the sequences was also analyzed against publicly available nematode genomes at Wormbase ParaSite database (<http://parasite.wormbase.org/>), with Phylum Nematoda. All BLASTp searches were carried out with a cutoff of $1e-05$ and bitscore >50. The characterization and prediction of the functional domains of ShK domain-containing proteins were carried out using the InterProScan database (<https://www.ebi.ac.uk/interpro/>) [45]. Secreted ShK domain-containing proteins were predicted based on the presence of signal peptide (SP) by SignalP (v5.0) [46] and InterProScan. The protein sequences of the ShK domain were downloaded from the UniProtKB database. From the list of 96 transcripts, a subset of 9 candidate genes encoding ShK domain-containing proteins were selected for further analysis due to the lack of identity with any other organism, indicating that these genes may be *B. xylophilus* specific. The sequences of the genes of interest in this study are available in v.1.3. of the *B. xylophilus* (BioProject PRJEA64437) [33]. To perform the phylogenetics analysis, multiple sequence alignment was performed using MAFFT (v.7.0) [47], followed by sequence trimming using trimAl (v.1.4.1) [48]. The phylogenetic trees were generated by two different methods: Neighbour Joining and Maximum-likelihood analysis (PhyML; in CLC Sequence mainWorkbench v.21, Qiagen) supported by 1,000 bootstrap replications. Phylogenetic trees were visualized and edited in iTOL (<https://itol.embl.de/>) [49].

4.3. Validation of the candidate genes

To validate the nine candidate genes in *B. xylophilus* genome and transcriptome, primers were designed to amplify full-length sequences by PCR with Supreme NZYTaq II 2x green master mix (NZYTech, Portugal). DNA extraction was performed using NZY Tissue gDNA Isolation kit (NZYTech, Portugal), according to the manufacturer's instructions. The PCR reaction was performed with an initial denaturation step for 3 min at 95°C, followed by 35 cycles of denaturation for 30 s at 94 °C, annealing for 30 s at 55°C and extension for 30 s at 72°C, followed by a final extension step of 10 min at 72 °C. The amplified products were visualized in 1.4 % agarose gel and were purified by MinElute® PCR or Gel Extraction Kits (QIAGEN, Germany), according to the manufacturer's instructions, and sent for sequencing at STABvida (Costa da Caparica, Portugal). Sequencing results were analyzed at BioEdit [50].

4.4. Oxidative stress assay

The ShK domain-containing proteins with predictive expression in *B. xylophilus* were tested under oxidative stress with hydrogen peroxide (H₂O₂), in two different concentrations of 15 mM and 30 mM [35]. A 96-well plate was prepared as follows: each well received 50 µl of H₂O₂ and 50 µl of mixed-life stage nematode solution (approximately 280 nematodes per 50 µl of sterilized distilled water). A control treatment with distilled water was also prepared. For each treatment condition three technical replicas per experiment were prepared. After a 24-hour incubation at room temperature, the plate was examined under a stereomicroscope (Olympus SZX12) to check for animal viability.

4.5. RNA extraction and gene relative expression profile

Total RNA from 24h-stressed *B. xylophilus* was extracted from the three conditions (0 mM, 15 mM H₂O₂, 30 mM H₂O₂) using RNeasy Mini kit, following manufacturer's instructions (QIAGEN, Germany). The quantity and quality of the extracted RNA were assessed by a ND-2000/2000c NanoDrop spectrophotometer (Thermo Scientific), and 200 ng cDNA final concentration was synthesized using the SuperScript® III reverse transcriptase (Invitrogen, by Thermo Fisher Scientific). Prior to qRT-PCR, primers previously designed using Prime 3 software [51], were tested for specificity (Supp. data Table S2). Relative gene expression was analyzed by quantitative RT-PCR (qRT-PCR) using SYBR green assay SensiFAST™ SYBR Lo-ROX mix, 2x (Bioline) and performed using the QuantGene 9600 (Bioer Technology, China). The reaction mix comprised 10 µL of SYBR green assay, 0.8 µL of each 10 mM primer and 1 µL of cDNA (10ng/µL) in a final volume of 20 µL. For each treatment, three experimental replications were conducted and negative controls with no template were added for each qRT-PCR run. The amplification was performed with initial denaturation at 95°C for 2 mins; 39 cycles of denaturation at 95°C for 5 sec, annealing and extension at 60°C for 20 sec; followed by the melting stage. Primer specificity was confirmed by a single peak at the PCR product's melting point. Bxy-actin (BXY_0322900) was used as a reference gene for normalization according to the 2^{-ΔΔCT} method [52]. The data were analyzed with Ct (cycle threshold) values in control treatment (without H₂O₂) and oxidative stress conditions (15mM and 30mM H₂O₂). Statistical analyses were performed with Jamovi software (v.2.3.21) (<https://www.jamovi.org>) using analysis of variance (ANOVA), and means were compared using Tukey's test with statistical significance at p-value < 0.05.

4.6. In situ hybridization assay

To determine the spatial expression patterns of candidate genes, *in situ* hybridization using digoxigenin (DIG)-labeled probes was performed based on the protocol described by [53]. Total RNA from *B. xylophilus* was extracted, as previously described. cDNA was synthesized using 50 ng of total RNA by the SuperScript® III first-strand synthesis system for RT-PCR (Invitrogen by life technologies) following the manufacturer's instructions. For each gene, a specific fragment of approximately 150-250 bp was amplified by PCR. The primers used are shown in Supp. data Table S2. The amplification reaction mixture consisted of 1U Platinum® Taq DNA Polymerase High Fidelity (Invitrogen by Life technologies), 1 mM of each primer (forward and reverse), 10 mM of dNTPs and 50 ng of template cDNA in a 50 µl reaction volume. The PCR reaction was performed with an initial denaturation step for 3 min at 95°C, followed by 35 cycles of denaturation for 30 s at 94 °C, annealing for 30 s at 55°C and extension for 30 s at 72°C, followed by a final extension step of 10 min at 72 °C. The amplified products were visualized in 1.4 % agarose gel and were purified by MinElute® PCR or Gel Extraction Kits (QIAGEN, Germany). The resulting PCR products were used as a template for the generation of both, sense and antisense, DIG-labeled probes using a DIG DNA Labeling Mix (Roche). The antisense probe is synthesized with the primer reverse and is complementary to the transcript mRNA sequence of interest, opposite to the sense probe synthesized with the primer forward (which will not hybridize with the mRNA) and used as a negative control. The probe synthesis (each per transcript) was performed with more than 50 ng of amplified specific fragments. A reaction was performed with an initial polymerase activation step for 2 min at 95 °C, followed by 35 cycles of denaturation for 15 s at 95 °C, annealing for 30 s at 50 °C and extension for 90 s at 72 °C, followed by a final extension step of 5 min at 72 °C. For the mRNA *in situ* hybridization in the nematode's tissues, mixed life stage *B. xylophilus* were fixed overnight in 2% (wt/vol) paraformaldehyde and cut using a vibrating aquarium air pump with a razor blade vertically on the slide, moved slowly back and forth across the nematode suspension. Nematodes were pre-treated with proteinase K for 30 min at room temperature in the rotator and hybridized for 16hrs, at 49°C, with both sense and antisense probes for each candidate transcript. Then, hybridized nematode tissues were detected using anti-Digoxigenin-AP FAB fragments (Roche) conjugated to alkaline phosphatase detection buffer and its substrate, NBT/BCIP Stock Solution (Roche). Nematode

segments were observed using a light microscope (Olympus BX50) and images were taken using the software CellP 3.2 (Olympus Soft Imaging Solutions).

Supplementary Materials: The following supporting information can be downloaded at the website of this paper posted on Preprints.org, Table S1: List of NCBI accessions used for multiple sequence alignment and phylogenetics inference. Table S2: List of primers used in this study for qRT-PCR and validation of the full-length transcripts.

Author Contributions: “Conceptualization, M.E.; methodology, M.E., C.L.V.; validation, writing—original draft preparation, M.E., M.M., C.S.L.V.; writing—review and editing, M.E., M.M., C.L.V.; funding acquisition, M.E. All authors have read and agreed to the published version of the manuscript.”

Funding: This research was funded by National Funds from FCT, Portuguese Foundation for Science and Technology, under the project PTDC/ASP-PLA/1108/2021 (NemaWAARS). M.E. was funded by CEECIND/00066/2018, C.S.L.V. was funded by CEECIND/00040/2018 and M.M. was supported by PTDC/ASP-PLA/1108/2021 (NemaWAARS), DOI: 10.54499/PTDC/ASP-PLA/1108/2021.

Conflicts of Interest: The authors declare no conflict of interest.

References

- Boyd, I.L.; Freer-Smith, P. H.; Gilligan, C. A.; Godfray, H.C.J. The Consequence of Tree Pests and Diseases for Ecosystem Services. *Science*, **2013**, *342*, 1235773. DOI: 10.1126/science.1235773.
- Jones, J.T.; Haegeman, A.; Danchin, E.G.J.; Gaur, H.S.; Helder, J.; Jones, M.G.K.; Kikuchi, T.; Manzanilla-López, R.; Palomares-Rius, E.J.; Wesemael, W.M.L.; Perry, R.N. Top 10 plant-parasitic nematodes in molecular plant pathology. *Molecular plant pathology*, **2013**, *14*, 946-961. DOI: 10.1111/mpp.12057.
- EPPO Bulletin. **2023**. PM 7/4 (4) *Bursaphelenchus xylophilus*. DOI: 10.1111/epp.12915.
- Mamiya, Y. Pathology of the pine wilt disease caused by *Bursaphelenchus xylophilus*. *Annual review of Phytopathology* **1983**, *21*, 201-220. DOI: 10.1146/annurev.py.21.090183.001221.
- Mota, M.M.; Braasch, H.; Bravo, M.A.; Penas, A.C.; Burgermeister, W.; Metge, K.; Sousa, E. First report of *Bursaphelenchus xylophilus* in Portugal and in Europe. *Nematology* **1999**, *1*, 727-734. DOI: 10.1163/156854199508757.
- Robertson, L.; Cobacho Arcos, S.; Escuer, M.; Santiago Merino, R.; Esparrago, G.; Abelleira, A.; Navas, A. Incidence of the pinewood nematode *Bursaphelenchus xylophilus* Steiner & Buhner, 1934 (Nickle, 1970) in Spain. *Nematology* **2011**, *13*, 6, 755-757. DOI: 10.1163/138855411X578888755.
- Vicente, C.S.L.; Espada, M.; Vieira, P.; Mota, M. Pine wilt disease: a threat to European forestry. *Eur. J. Plant Pathol.* **2012**, *133*, 89-99. DOI: 10.1007/s10658-011-9924-x.
- Vieira, P.; Gleason, C. Plant-parasitic nematode effectors - insights into their diversity and new tools for their identification. *Curr Opin Plant Biol.* **2019**, *50*, 37-43. DOI: 10.1111/epp.12915.
- Espada, M.; Silva, A.C.; Eves-van den Akker, S.; Cock, P.J.A.; Mota, M.; Jones, J.T. Identification and characterization of parasitism genes from the pinewood nematode *Bursaphelenchus xylophilus* reveals a multi-layered detoxification strategy. *Molecular Plant Pathology* **2016**, *17*, 286-295. DOI: 10.1111/mpp.12280.
- Tsai, I.J.; Tanaka, R.; Kanzaki, N.; Akiba, M.; Yokoi, T.; Espada, M.; Jones, J.T.; Kikuchi, T. Transcriptional and morphological changes in the transition from mycetophagous to phytophagous phase in the plant-parasitic nematode *Bursaphelenchus xylophilus*. *Molecular Plant Pathology* **2016**, *17*, 77-83. DOI: 10.1111/mpp.12261.
- Rangaraju, S.; Khoo, K.; Feng, Z.P.; Crossley, G.; Nugent, D.; Khaytin, I.; Chi, V.; Pham, C.; Calabresi, P.; Pennington, M.; Norton, R.; Chandy, G. Potassium Channel Modulation by A Toxin Domain in Matrix Metalloprotease 23. *The Journal of biological chemistry* **2009**, *285*, 12, 9124-9136. DOI: 10.1074/jbc.M109.071266.
- Castañeda, O.; Sotolongo, V.; Amor, A.M.; Stöcklin, R.; Anderson, A.J.; Harvey, A.L.; Engström, A.; Wernstedt, C.; Karlsson, E.; Characterization of a potassium channel toxin from the Caribbean Sea anemone *Stichodactyla helianthus*. *Toxicon* **1995**, *33*, 5, 603-13. DOI: 10.1016/0041-0101(95)00013-c.
- Cotton, J.; Crest, M.; Bouet, F.; Alessandri, N.; Gola, M.; Forest, E.; Karlsson, E.; Castañeda, O.; Harvey, A.L.; Vita, C.; Ménez, A. *Eur. J. Biochem.* **1997**, *244*, 192-202. DOI: 10.1111/j.1432-1033.1997.00192.x.
- Tudor, J.E.; Pallaghy, P.K.; Pennington, M.W.; Norton, R.S. Solution structure of ShK toxin, a novel potassium channel inhibitor from a sea anemone. *Nat. Struct. Biol.* **1996**, *3*, 317-320. DOI: 10.1038/nsb0496-317.
- Loukas, A.; Hintz, M.; Linder, D.; Mullin, N.P.; Parkinson, J.; Tetteh, K.K.; Maizels, R.M. A family of secreted mucins from the parasitic nematode *Toxocara canis* bears diverse mucin domains but shares similar flanking six-cysteine repeat motifs. *J. Biol. Chem.* **2000**, *275*, 39600-39607. DOI: 10.1074/jbc.M005632200.

16. Prentis, P.J.; Pavasovic, A.; Norton, R.S. Sea Anemones: Quiet Achievers in the Field of Peptide Toxins. *Toxins* **2018**, *10*, 30. DOI: 10.3390/toxins10010036.
17. von Reumont, B.M.; Campbell, L.I.; Richter, S.; Hering, L.; Sykes, D.; Hetmank, J.; Jenner, R.A.; Bleidorn, C. A Polychaete's powerful punch: venom gland transcriptomics of *Glycera* reveals a complex cocktail of toxin homologs. *Genome Biol Evol.* **2014**, *6*, 9, 2406-2423. DOI: 10.1093/gbe/evu190.
18. Verdes, A.; Simpson, D.; Holford, M. Are Fireworms Venomous? Evidence for the Convergent Evolution of Toxin Homologs in Three Species of Fireworms (Annelida, Amphinomididae). *Genome Biol. Evol.* **2018**, *10*, 249-268. DOI: 10.1093/gbe/evx279.
19. Gerdol, M.; Cervelli, M.; Mariottini, P.; Oliverio, M.; Dutertre, S.; Modica, M.V. A Recurrent Motif: Diversity and Evolution of ShKT Domain Containing Proteins in the Vampire Snail *Cumia reticulata*. *Toxins* **2019**, *11*, 106. DOI: 10.3390/toxins11020106.
20. Suh, J.; Hutter, H. A survey of putative secreted and transmembrane proteins encoded in the *C. elegans* genome. *BMC Genomics* **2012**, *13*, 333. DOI: 10.1186/1471-2164-13-333.
21. Lima, A.K.; Dhillon, H.; Dillman, A.R. ShK-Domain-Containing Protein from a Parasitic Nematode Modulates *Drosophila melanogaster* Immunity. *Pathogens* **2022**, *11*, 1094. DOI: 10.3390/pathogens11101094.
22. Frias, J.; Toubarro, D.; Bjerga, G.E.K.; Puntervoll, P.; Vicente, J.B.; Reis, R.L.; Simões, N. A ShK-like Domain from *Steinernema carpocapsae* with Bioinsecticidal Potential. *Toxins* **2022**, *14*, 754. DOI: 10.3390/toxins14110754.
23. Vieira, P.; Myers, R.Y.; Pellegrin, C.; Wram, C.; Hesse, C.; Maier, T.; Shao, J.; Koutsovoulos, G.D.; Zasada, I.; Matsumoto, T.; Danchin, E.; Baum, T.J.; Eves-van den Akker, S.; Nemchinov, L.G. Targeted transcriptomics reveals signatures of large-scale independent origins and concerted regulation of effector genes in *Radopholus similis*. *PLoS Pathog.* **2021**, *17*, 11: e1010036. DOI: 10.1186/1471-2164-13-333.
24. Vieira, P.; Shao, J.; Vijayapalani, P.; Maier, T.; Pellegrin, C.; Eves-van den Akker, S.; Baum, T.J.; Nemchinov, L. A new esophageal gland transcriptome reveals signatures of large scale de novo effector birth in the root lesion nematode *Pratylenchus penetrans*. *BMC Genomics* **2020**, *21*, 738. DOI: 10.1186/s12864-020-07146-0.
25. Kumar, A.; Fitoussi, N.; Sanadhya, P.; Sichov, N.; Bucki, P.; Bornstein, M.; Belausov, E.; Miyara, B. S. Two Candidate *Meloidogyne javanica* Effector Genes, *MjShKT* and *MjPUT3*: A Functional Investigation of Their Roles in Regulating Nematode Parasitism. *Molecular Plant-Microbe Interactions* **2023**, *36*, 2, 79-94. DOI: 10.1094/MPMI-10-22-0212-R.
26. Habash, S.S.; Radakovic, Z.S.; Vankova, R.; Siddique, S.; Dobrev, P.; Gleason, C.; Grundler, F.M.W.; Elashry, A. *Heterodera schachtii* Tyrosinase-like protein - a novel nematode effector modulating plant hormone homeostasis. *Sci Rep.* **2017**, *7*, 6874. DOI: 10.1038/s41598-017-07269-7.
27. Cantacessi, C.; Mitreva, M.; Campbell, B.E.; Hall, R.S.; Young, N.D.; Jex, A.R.; Ranganathan, S.; Gasser, R.B. First transcriptomic analysis of the economically important parasitic nematode, *Trichostrongylus colubriformis*, using a next-generation sequencing approach. *Infection, Genetics and Evolution* **2010**, *10*, 8, 1199-1207. DOI: 10.1016/j.meegid.2010.07.024.
28. Cahalan, M.D.; Chandy, K.G. The functional network of ion channels in T lymphocytes. *Immunol Rev.* **2009**, *231*, 1, 59-87. DOI: 10.1111/j.1600-065X.2009.00816.x.
29. Beeton, C.; Pennington, M.W.; Norton, R.S.; Analogs of the Sea Anemone Potassium Channel Blocker ShK for the Treatment of Autoimmune Diseases. *Inflamm Allergy Drug Targets* **2011**, *10*, 5, 313-321. DOI: 10.2174/187152811797200641.
30. Chhabra, S.; Chang, S.C.; Nguyen, H.M.; Huq, R.; Tanner, M.R.; Londono, L.M.; Estrada, R.; Dhawan, V.; Chauhan, S.; Upadhyay, S.K.; Gindin, M.; Hotez, P.J.; Valenzuela, J.G.; Mohanty, B.; Swarbrick, J.D.; Wulff, H.; Iadonato, S.P.; Gutman, G.A.; Beeton, C.; Pennington, M.W.; Norton, R.S.; Chandy, K.G. Kv1.3 channel-blocking immunomodulatory peptides from parasitic worms: Implications for autoimmune diseases. *FASEB J.* **2014**, *28*, 3952-3964. DOI: 10.1096/fj.14-251967.
31. Dreyer, I.; Uozumi, N. Potassium channels in plant cells. *The FEBS Journal* **2011**, *278*, 4293-4303. DOI: 10.1111/j.1742-4658.2011.08371.x.
32. Joshi, I., Kumar, A., Singh, A.K. *et al.* Development of nematode resistance in Arabidopsis by HD-RNAi-mediated silencing of the effector gene *Mi-msp2*. *Sci Rep.* **2019**, *9*, 17404. DOI: 10.1038/s41598-019-53485-8.
33. Kikuchi, T.; Cotton, J.A.; Dalzell, J.J.; Hasegawa, K.; Kanzaki, N.; McVeigh, P.; Takahashi, T.; Tsai, I.J.; Assefa, S.A.; Cock, P.J.A.; Otto, T.D.; Hunt, M.; Reid, A.J.; Sanchez-Flores, A.; Tsuchihara, K.; Yokoi, T.; Larsson, M. C.; Miwa, J.; Maule, A.G.; Sahashi, N.; Jones, J.T.; Berriman, M. Genomic insights into the origin of parasitism in the emerging plant pathogen *Bursaphelenchus xylophilus*. *PLoS Pathog.* **2011**, *7*:e1002219. DOI: 10.1111/mpp.12261.
34. Tanaka, S.E.; Dayi, M.; Maeda, Y.; Tsai, I.J.; Tanaka, R.; Bligh, M.; Takeuchi-Kaneko, Y.; Fukuda, K.; Kanzaki, N.; Kikuchi, T. Stage-specific transcriptome of *Bursaphelenchus xylophilus* reveals temporal regulation of effector genes and roles of the dauer-like stages in the lifecycle. *Sci Rep.* **2019**, *9*, 6080. DOI: 10.1038/s41598-019-42570-7.

35. Vicente, C.S.L.; Ikuyo, Y.; Shinya, R.; Mota, M.; Hasegawa, K. Catalases Induction in High Virulence Pinewood Nematode *Bursaphelenchus xylophilus* under Hydrogen Peroxide-Induced Stress. *PLoS ONE* **2015**, *10*, 4: e0123839. DOI: 10.1371/journal.pone.0123839.
36. McNeilly, T.N.; Frew, D.; Burgess, S.T.G.; Wright, H.; Bartley, D.J.; Bartley, Y.; Nisbet, A.J. Niche-specific gene expression in a parasitic nematode; increased expression of immunomodulators in *Teladorsagia circumcincta* larvae derived from host mucosa. *Sci Rep.* **2017**, *7*, 7214. DOI: 10.1038/s41598-017-07092-0.
37. Espada, M.; Eves-van den Akker, S.; Maier, T.; Paramasivan, V.; Baum, T.J.; Mota, M.; Jones J.T. STATAWAARS: a promoter motif associated with spatial expression in the major effector-producing tissues of the plant-parasitic nematode *Bursaphelenchus xylophilus*. *BMC Genomics* **2018**, *19*:553. DOI: 10.1186/s12864-018-4908-2.
38. Columbus-Shenkar, Y.Y.; Sachkova, M.Y.; Macrander, J.; Fridrich, A.; Modepalli, V.; Reitzel, A.M.; Sunagar, K.; Moran, Yehu, M. Dynamics of Venom Composition Across a Complex Life Cycle. *Elife* **2018**, *7*:e35014. DOI: 10.7554/eLife.35014.
39. Schafer, W. Nematode nervous systems. *Current Biology* **2016**, *26*, 937–980. DOI: 10.1016/j.cub.2016.07.044.
40. Espada, M.; Jones, J.T.; Mota, M. Characterization of glutathione S-transferases from the pine wood nematode, *Bursaphelenchus xylophilus*. *Nematology* **2016**, *18*, 6, 697-709. DOI: 10.1163/15685411-00002985.
41. Evans, A.A.F. Mass culture of mycophagous nematodes. *J. Nematol.* **1970**, *2*, 99–100.
42. Southey, J.F. *Laboratory Methods for Work with Plant and Soil Nematodes* **1986**, London: Ministry of Agriculture Fisheries and Food, HMSO.
43. McGinnis S, Madden TL. BLAST: at the core of a powerful and diverse set of sequence analysis tools. *Nucleic Acids Res.* **2004**, *32*, 20–25. DOI: 10.1093/nar/gkh435.
44. Boratyn, G.M.; Camacho, C.; Cooper, P.S.; Coulouris, G.; Fong, A.; Ma, N.; Madden, T.L.; Matten, W.T.; McGinnis, S.D.; Merezhuk, Y.; Raytselis, Y.; Sayers, E.W.; Tao, T.; Ye, J.; Zaretskaya, I. BLAST: a more efficient report with usability improvements. *Nucleic Acids Res.* **2013**, *41*, 29-33. DOI: 10.1093/nar/gkt282.
45. Blum, M.; Chang, H.; Chuguransky, S.; Grego, T.; Kandasaamy, S.; Mitchell, A.; Nuka, G.; Paysan-Lafosse, T.; Qureshi, M.; Raj, S.; Richardson, L.; Salazar, G.A.; Williams, L.; Bork, P.; Bridge, A.; Gough, J.; Haft, D.H.; Letunic, I.; Marchler-Bauer, A.; Mi, H.; Natale, D.A.; Necci, M.; Orengo, C.A.; Pandurangan, A.P.; Rivoire, C.; Sigrist, C.J.A.; Sillitoe, I.; Thanki, N.; Thomas, P.D.; Tosatto, S.C.E.; Wu, C.H.; Bateman, A.; Finn, R.D. The InterPro protein families and domains database: 20 years on. *Nucleic Acids Research* **2020**, *49*, 344–354. DOI: 10.1093/nar/gkaa977.
46. Teufel, F.; Almagro Armenteros, J.J., Johansen, A.R.; Gíslason, M.H.; Pihl, S.I.; Tsirigos, K.D.; Winther, O.; Brunak, S.; von Heijne, G.; Nielsen, H. SignalP 6.0 predicts all five types of signal peptides using protein language models. *Nat Biotechnol.* **2022**, *40*, 1023–1025. DOI: 10.1038/s41587-021-01156-3.
47. Katoh, K.; Standley, D. MAFFT multiple sequence alignment software version 7: improvements in performance and usability. *Mol. Biol. Evol.* **2013**, *30*, 772–780. DOI: 10.1093/molbev/mst010
48. Capella-Gutiérrez, S.; Silla-Martínez, J.M.; Gabaldón, T. trimAl: a tool for automated alignment trimming in large-scale phylogenetic analyses. *Bioinformatics* **2009**, *25*, 1972–1973. DOI: 10.1093/bioinformatics/btp348.
49. Letunic, I.; Bork, P. Interactive Tree Of Life (iTOL) v5: an online tool for phylogenetic tree display and annotation, *Nucleic Acids Research* **2021**, *49*, 1, 293–296. DOI: 10.1093/nar/gkab301.
50. Hall, T.A. BioEdit: A User-Friendly Biological Sequence Alignment Editor and Analysis Program for Windows 95/98/NT. *Nucleic Acids Symposium Series* **1999**, *41*, 95-98. DOI: 10.14601/phytopathol_mediterr-14998u1.29.
51. Untergasser, A.; Cutcutache, I.; Koressaar, T.; Ye, J.; Faircloth, B.C.; Remm, M.; Rozen, S.G. Primer3—new capabilities and interfaces. *Nucleic Acids Research* **2012**, *40*. DOI: 10.1093/nar/gks596
52. Livak, K.J.; Schmittgen, T.D. Analysis of relative gene expression data using real-time quantitative PCR and the 2- $\Delta\Delta$ CT method. *Methods* **2001**, *25*, 402–408. DOI: 10.1006/meth.2001.1262.
53. de Boer, J.M.; Yan, Y.; Smant, G.; Davis, E.L.; Baum, T.J. *In-situ* hybridization to messenger RNA in *Heterodera glycines*. *J Nemat.* **1998**, *30*, 309–12.

Disclaimer/Publisher's Note: The statements, opinions and data contained in all publications are solely those of the individual author(s) and contributor(s) and not of MDPI and/or the editor(s). MDPI and/or the editor(s) disclaim responsibility for any injury to people or property resulting from any ideas, methods, instructions or products referred to in the content.